INFECTION AND IMMUNITY, Mar. 2001, p. 1329–1336 Vol. 69, No. 3
0019-9567/01/$04.00+0 DOI: 10.1128/IAI.69.3.1329–1336.2001

Clostridium difficile Toxins Disrupt Epithelial Barrier Function by Altering Membrane Microdomain Localization of Tight Junction Proteins

A. NUSRAT,[1]* C. VON EICHEL-STREIBER,[2] J. R. TURNER,[3,4] P. VERKADE,[5] J. L. MADARA,[1] AND C. A. PARKOS,[1]

Epithelial Pathobiology Research Unit, Department of Pathology, Emory University School of Medicine, Atlanta, Georgia[1]; Institut fur Medizinische Mikrobiologie und Hygiene, Universität Mainz, Mainz,[2] Cell Biology and Biophysics Program, EMBL, Heidelberg,[3] and Max Planck Institute of Molecular Cell Biology and Genetics, Dresden,[4] Germany; and Department of Pathology, Wayne State University, Detroit, Michigan[5]

Received 28 July 2000/Returned for modification 14 September 2000/Accepted 20 November 2000

The anaerobic bacterium *Clostridium difficile* is the etiologic agent of pseudomembranous colitis. *C. difficile* toxins TcdA and TcdB are UDP-glucosyltransferases that monoglucosylate and thereby inactivate the Rho family of GTPases (W. P. Ciesla, Jr., and D. A. Bobak, J. Biol. Chem. 273:16021–16026, 1998). We utilized purified reference toxins of *C. difficile*, TcdA-10463 (TcdA) and TcdB-10463 (TcdB), and a model intestinal epithelial cell line to characterize their influence on tight-junction (TJ) organization and hence to analyze the mechanisms by which they contribute to the enhanced paracellular permeability and disease pathophysiology of pseudomembranous colitis. The increase in paracellular permeability induced by TcdA and TcdB was associated with disorganization of apical and basal F-actin. F-actin restructuring was paralleled by dissociation of occludin, ZO-1, and ZO-2 from the lateral TJ membrane without influencing the subjacent adherens junction protein, E-cadherin. In addition, we observed decreased association of actin with the TJ cytoplasmic plaque protein ZO-1. Differential detergent extraction and fractionation in sucrose density gradients revealed TcdB-induced redistribution of occludin and ZO-1 from detergent-insoluble fractions constituting "raft-like" membrane microdomains, suggesting an important role of Rho proteins in maintaining the association of TJ proteins with such microdomains. These toxin-mediated effects on actin and TJ structure provide a mechanism for early events in the pathophysiology of pseudomembranous colitis.

Clostridium difficile is an anaerobic bacterium that is a causative agent of antibiotic-associated diarrhea. Disease etiology is primarily linked to the bacterial production of two exotoxins referred to as toxins A and B. *C. difficile* toxins A and B, also referred to as TcdA-10463 (TcdA) and TcdB-10463 (TcdB), are large monomeric proteins toxins that have ~45% amino acid identity and have M_rs of 308,000 and 270,000, respectively (50). Although the precise mechanisms by which these toxins induce disease are incompletely understood, the intracellular targets of the toxins in epithelial cells have been well described. Both toxins disrupt the function of the Rho family of low-molecular-weight GTP binding proteins including Rho, Rac, Cdc42, and Rap in the case of TcdA. They do so by using UDP-glucose as a cosubstrate and monoglucosylating these proteins (1, 10, 24, 25). Since Rho, Rac, and Cdc42 play a crucial role in regulating the organization of the actin cytoskeleton (17), their inactivation is associated with dysregulation of the cytoskeletal network. The *C. difficile* toxins have been previously documented to influence barrier function in intestinal epithelial cells (19, 20). In addition, we have previously utilized a chimeric DC3B toxin that specifically ADP-ribosylates and inactivates Rho function without influencing Rac and Cdc42. Incubation of epithelial cells with DC3B was associated with altered apical F-actin organization and disruption of epithelial barrier function (34). While the molecular basis of these observations is not known, it is clear that the apical perijunction F-actin ring is closely associated with tight junctions (TJs) (31). TJs play an important regulatory role in barrier function, and numerous proteins have been identified in this region. For example, occludin and claudin(s) are integral membrane proteins believed to associate with the apical perijunction F-actin ring via cytoplasmic plaque proteins such as ZO-1 (11, 13–15, 40, 47, 48). The hyperphosphorylated form of occludin that is of high molecular weight (HO) is believed to represent a key functional component of the TJ (54). Recent evidence suggests that the functional components of TJs partition into specific membrane microdomains (36). Utilizing a differential detergent extraction and sucrose density gradient approach, we have recently shown that HO and ZO-1 reside in membrane microdomains with characteristics of membrane "rafts" or detergent-insoluble glycolipid rafts (DIGs) (36). Such "Raft"-like membrane microdomains contain sphingolipid and cholesterol assemblies and serve to recruit specific membrane proteins. These cholesterol-enriched membrane domains have previously been defined on the basis of biochemical isolation properties and more recently by utilizing fluorescence resonance energy transfer microscopy and chemical cross-linking studies (2, 4, 5, 7, 12, 18, 41, 43, 49). Other important cellular components associated with glycolipid rafts include signal trans-

* Corresponding author. Mailing address: Department of Pathology and Laboratory Medicine, Emory University, WMRB 2335, 1639 Pierce Dr., Atlanta, GA 30322. Phone: (404) 727-8543. Fax: (404) 727-3321. E-mail: anusrat@emory.edu.

duction proteins and a 21 to 24-kDa scaffolding protein, caveolin. For example, we have recently observed that caveolin-1 focally coassociates with occludin in functionally intact TJs (36).

From the above observations, it is clear that the relationship of structural elements of TJ with the actin cytoskeleton is complex and highly regulated. There is abundant evidence that key regulatory elements include both the heterotrimeric GTP binding proteins and the small GTP binding proteins of the Rho and Rab subfamilies (9, 23, 34, 52). In this study we examined the effects of TcdA and TcdB on TJ structure and function in model T84 intestinal epithelial cells. Such studies will shed further light on the influence of Rho-inactivating toxins on TJ structure and function. T84 cells have phenotypic characteristics of crypt intestinal epithelial cells and form well-developed TJs when grown as a monolayer (33). Incubation of T84 monolayers with TcdA or TcdB was associated with marked changes in F-actin organization and TJ disruption. A key cytoplasmic plaque TJ protein, ZO-1, was displaced from a Triton X-100 (TX-100)-insoluble raft containing membrane microdomain to a TX-100-soluble pool, and a decrease in high-molecular-weight occludin was observed following incubation of T84 monolayers with the TcdA and TcdB toxins. The TcdAB-induced effects on TJ structure and function were paralleled by disorganization of F-actin in the apical and basal poles of epithelial cells. The global disorganization of F-actin induced by TcdAB contrasts with the effects of another bacterial toxin, C3 transferase, which specifically ADP-ribosylates Rho and influences the apical F-actin pool and TJ function. Our results suggest that the TcdAB toxins either directly or indirectly influence TJ function and modulate both the membrane microdomain localization of TJ proteins and the affiliation of TJs with the underlying actin cytoskeleton.

MATERIALS AND METHODS

Cell culture and electrophysiology. T84 cells (ATCC CCL-248) were passaged and grown on collagen-coated permeable supports as previously described (33, 38). Cells (passages 50 to 90) were grown in a 1:1 mixture of Dulbecco's modified Eagle's medium and Ham's F-12 medium supplemented with 15 mM HEPES buffer (pH 7.5), 14 mM $NaHCO_3$, 40 μg of penicillin per ml, 8 μg of ampicillin per ml, 90 μg of streptomycin per ml, and 5% newborn calf serum.

C. difficile reference toxins TcdA-10463 (TcdA) and TcdB-10463 (TcdB) were purified and utilized for these studies (24, 25). Monolayers were incubated with TcdA and TcdB in serum-free, antibiotic-free cell culture medium and applied to the apical and basolateral surfaces of epithelial cells. Control monolayers were incubated with serum-free, antibiotic-free cell culture medium only.

Transepithelial resistance to passive ion flow was measured as described previously (30, 37, 38, 44). The apical and basolateral reservoirs of monolayers grown on filters were connected to calomel and Ag-AgCl electrodes via agar bridges. A voltage clamp was used to determine the voltage response to a current pulse of 25 μA. Transepithelial resistance was then calculated using Ohm's law. Sieving characteristics of monolayers was examined by flux studies using the radiolabeled extracellular space marker mannitol (3.6 Å). [^{3}H] mannitol was added to the apical chamber of monolayers accompained by excess cold tracer to both sides of the monolayer. Fluid aliquots were obtained from the "cold" side every 20 min for 120 min under control (medium-only) and experimental (Tcd-incubated monolayers) conditions. Samples were taken from the "hot" side of monlayers at the end of each experiment. Samples were then added to scintillation fluid and counted. The unidirectional flux, J, was determined by J = dpm/(specific activity × surface area × incubation time) (32).

Immunoprecipitation and Western blotting. ZO-1, actin, and occludin were immunoprecipitated from TcdB-incubated and control (medium-only) T84 monolayers with polyclonal antibodies (Zymed, Inc., and Sigma) and protein A-Sepharose, using solubilized cell lysate as described below. Briefly, monolayers grown to confluence on 5-cm^2 permeable supports were isolated by scraping with a Teflon spatula into Hanks balanced salt solution (HBSS) containing 1% *n*-octylglucoside with protease inhibitors, followed by low-speed centrifugation (2,000 × *g*; Beckman GS-6R centrifuge) for 10 min. Cell extracts were subsequently incubated with primary antibodies (~10 μg/ml) for 3 h at 4°C followed by protein A-Sepharose (Pharmacia, Piscataway, N.J.) (20 μl of beads) for 3 h at 4°C. Immunoprecipitated proteins were denatured in sample buffer and subjected to sodium dodecyl sulfate-polyacrylamide gel electrophoresis and Western blotting using standard methods as previously described (21, 35).

Isolation of detergent-insoluble glycolipid rafts by sucrose gradient fractionation. T84 cells were grown on 45-cm^2 permeable supports (33) and incubated with or without TcdB (80 ng/ml) for 2 h in cell culture medium. Two confluent monolayers per condition were rinsed in HBSS, and cells were isolated by scraping with a Teflon spatula into HBSS containing 1% TX-100 and protease inhibitors (5 mM diisopropylfluorophosphate, 1.25 μM phenylmethylsulfonyl fluoride, 10 μg each of leupeptin and chymostatin per ml, 10ug/ml and 10 μM aprotinin) and homogenized using a Dounce homogenizer. After the sucrose concentration of the lysate was adjusted to 40%, it was placed in the bottom of an ultracentrifuge tube and overlaid with a 5 to 30% (weight/weight) linear sucrose gradient as previously described (36). The gradients were subjected to ultracentrifugation (19 h at 39,000 rpm at 4°C) in a Beckman SW41 rotor, fractionated, and analyzed for sucrose concentration, light scattering at 600 nm, and alkaline phosphatase activity by previously described procedures (5, 26, 41, 53). Distribution of TJ proteins (ZO-1 and occludin) and the membrane raft (DIG)-associated protein caveolin-1 was determined by sodium dodecyl sulfate-polyacrylamide gel electrophoresis and Western blotting. Antibodies to the above proteins were obtained from Zymed Inc., Transduction Labs, and Santa Cruz, respectively.

Immunofluorescence, immunogold labeling, and electron microscopy. Monolayers of T84 cells were washed in HBSS, fixed in ethanol at −20°C for 20 min, incubated with the respective primary antibodies to occludin, ZO-1, or ZO-2 for 60 min in a humidity chamber, washed, and incubated with fluorescein isothiocyanate-conjugated secondary antibodies (Jackson Labs). Monolayers mounted in *p*-phenylenediamine glycerol (1:1) were analyzed by confocal laser microscopy (Zeiss dual laser confocal microscope model 1510).

Monolayers were processed for electron microscopy and imaged as previously described (33). For immunogold labeling, filter-grown confluent T84 monolayers were rinsed in HBSS and fixed with 3.7% paraformaldehyde–HBSS (PFA) for 10 min. Filters were progressively infiltrated with gelatin at 37°C to a final concentration of 10%. The gelatin was solidified on ice, and small pieces were cut from the filter, infiltrated with 2.1 M sucrose put on a stub, and frozen in liquid nitrogen, and ultrathin cryosections were collected on grids. The grids were subsequently incubated for 1 h each at room temperature with purified caveolin-1 polyclonal antibodies (1:20) and protein A-coupled 10-nm gold particles. The grids were rinsed, fixed in 4% PFA, and incubated with polyclonal antibody to occludin (1:400) for 1 h followed by protein A-coupled 15-nm gold particles for 1 h at room temperature. The grids were rinsed and incubated for 5 min on ice in 0.3% uranyl acetate–1.8% methylcellulose in tridistilled water (5 min at 4°C). Excess fluid was removed, and grids were air dried and analyzed. Controls included omission of primary antibodies.

RESULTS

***C. difficile* toxins enhance paracellular permeability in epithelial monolayers.** We utilized previously characterized reference toxins. TcdA and TcdB, for our studies (24, 25, 51). These toxins induced a profound drop in transepithelial resistance within 2 h (Fig. 1). Dilution studies revealed a maximal fall in transepithelial resistance using 240 ng of TcdA per ml and 80 ng of TcdB per ml, suggesting that T84 cells are more sensitive to TcdB than to TcdA. The fall in transepithelial resistance was observed after application of TcdA or TcdB to either the apical or basolateral compartments. Time course experiments for the drop in transepithelial resistance were similar irrespective of apical or basolateral application of TcdAB. To determine if the drop in transepithelial resistance in toxin-treated monolayers (240 ng of TcdA per ml and 80 ng of TcdB per ml for 2 h) represented enhanced paracellular permeability, we undertook flux assays using radiolabeled mannitol. The cumulative transmonolayer flux of [^{3}H]mannitol

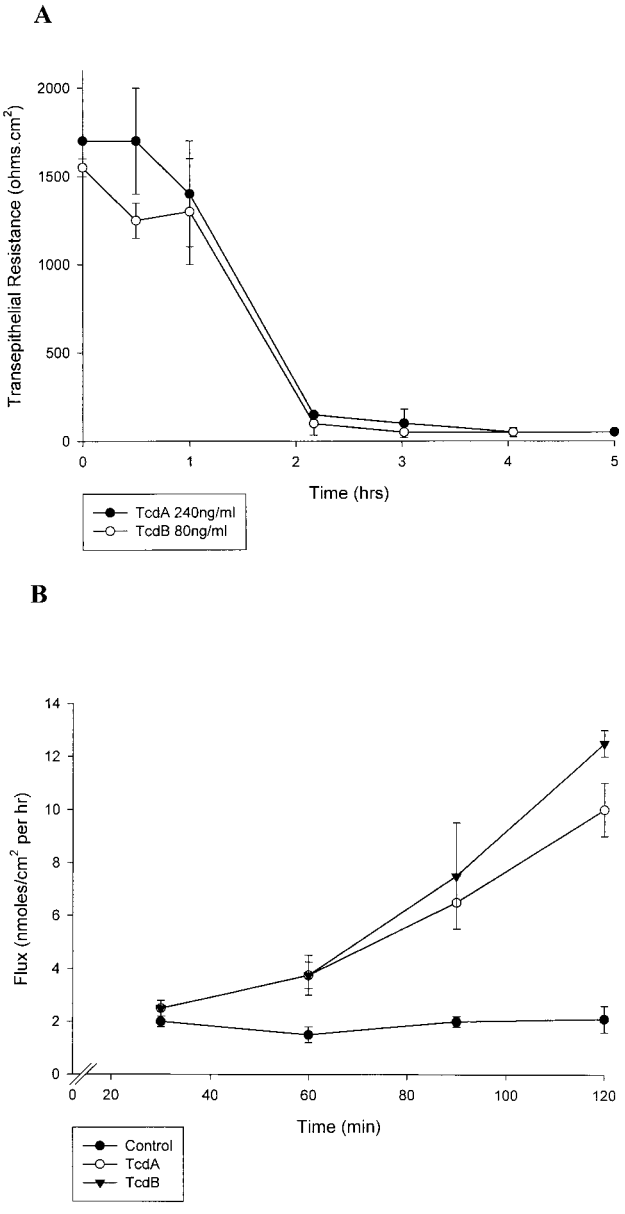

FIG. 1. *C. difficile* toxins enhance paracellular permeability of T84 epithelial monolayers. T84 monolayers were incubated with *C. difficile* toxin A-10463 (TcdA, 240 ng/ml) or B-10463 (TcdB, 80 ng/ml). (A) Time course experiments demonstrated a maximal fall in the transepithelial resistance in ~2 h. (B) The cumulative transmonolayer flux of radiolabled mannitol was measured after 60 min of TcdAB exposure. A markedly enhanced flux of mannitol was observed in monolayers incubated with Tcd toxins (B). Analogous to the resistance results, TcdB was more potent than TcdA in enhancing monolayer flux.

was significantly enhanced by both TcdA and TcdB (Fig. 1B), suggesting increased paracellular permeability. As mentioned above, we noted greater sensitivity of T84 cells to TcdB than to TcdA. These findings are in keeping with previous reports illustrating the influence of *C. difficile* toxins in other cell types (1, 6, 39). In particular, these studies documented an enhanced sensitivity of native intestinal epithelium to *C. difficile* toxin B compared to toxin A (~10 fold) and that TcdB-10463 is enzymatically more potent than TcdA-10463.

F-actin organization in both the apical and basal poles of epithelial cells is influenced by the *C. difficile* toxins. Given that TcdAB monoglucosylate and inactivate the actin regulating Rho proteins, we determined F-actin organization in T84 epithelial cells incubated with these toxins. Disruption of F-actin architecture was observed in parallel with the TcdAB-induced increase in paracellular permeability. Rhodamine phalloidin was utilized to highlight the F-actin organization. Representative en face confocal images of epithelial cells exposed to TcdB are shown in Fig. 2. While control epithelial monolayers had organized F-actin in the apical brush border/perijunctional actin ring and basal stress fibers, the TcdB monolayers exhibited disorganization and disruption of normal F-actin architecture. As can be seen in Fig. 2, both apical and basal F-actin structures were markedly altered by TcdB treatment. The earliest change in F-actin organization was observed within 1 h of TcdB incubation (80 ng of TcdB per ml). Such alterations were paralleled by a fall in transepithelial resistance. TcdA induced analogous effects on F-actin organization (data not shown).

Disassembly of tight junctions by the *C. difficile* toxins. Since TcdA and TcdB toxins enhanced paracellular permeability and induced disruption of apical F-actin, we determined the effect

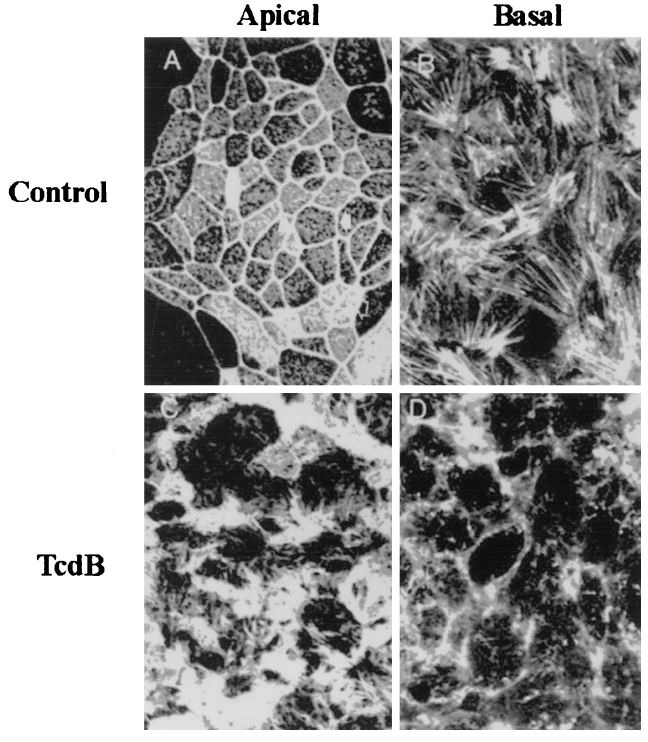

FIG. 2. *C. difficile* toxins influence F-actin architecture in the apical and basal poles of T84 intestinal epithelial cells. F-actin distribution in control (serum-free medium) (top panels) or TcdB (bottom panels)-exposed monolayers was determined 2 h after toxin incubation. Confocal microscopic localization of F-actin in en face optical sections reveals a normal F-actin distribution in the apical membrane and as perijunctional F-actin rings (top left). Prominent stress fibers are observed in the base of cells (top right). Incubation with this toxin induced disruption and disorganization of F-actin in both the apical (bottom left) and basal (bottom right) poles of T84 cells. Note the loss of apical perijunction F-actin rings and basal stress fibers. Representative data from six individual experiments are shown.

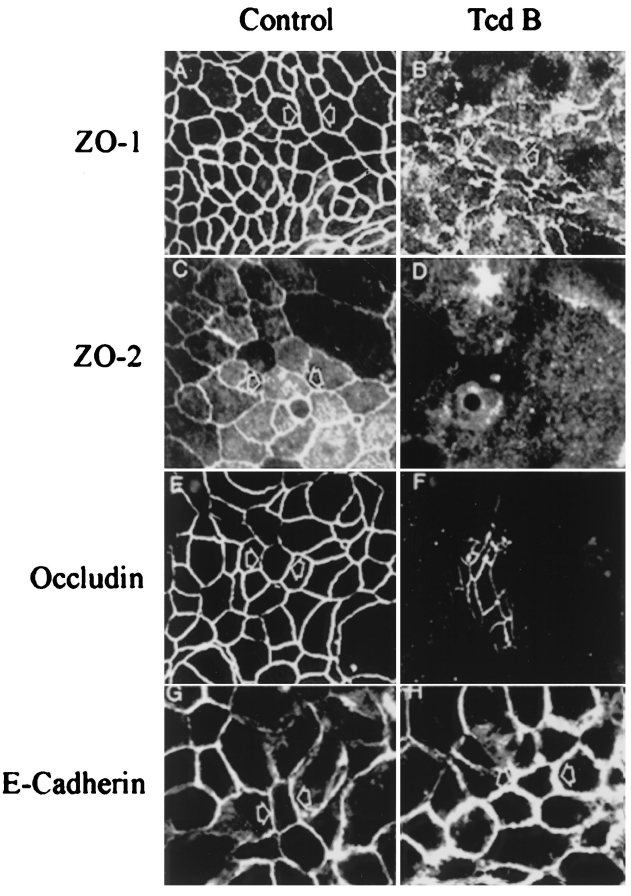

FIG. 3. Organization of tight junction structural proteins is influenced by *C. difficile* toxins. TJ proteins (ZO-1, ZO-2, and occludin) and AJ protein (E-cadherin) in control (medium only) or TcdB-exposed (2 h) monolayers were localized by immunofluorescence labeling and confocal microscopy. En face images in the apical region of epithelial cells reveal a normal "chicken wire" pattern of staining for ZO-1 (A), ZO-2 (C), and occludin (E) at TJs of control monolayers. TcdB exposure induced the displacement of ZO-1 (B), ZO-2 (D), and occludin (F) from the lateral membrane. However, distribution of E-cadherin in control monolayers (G) was indistinguishable from that in TcdB-exposed monolayers (H). Representative data from six individual experiments are shown.

of these toxins on distribution of TJ and adherens junction (AJ) proteins. TJ proteins ZO-1, ZO-2, occludin, and the AJ protein E-cadherin in control (medium only) and Tcd-exposed monolayers were immunolocalized by confocal microscopy (Fig. 3). In control monolayers, the TJ and AJ proteins immunolocalized as continuous rings. Following TcdB exposure, the TJ proteins were displaced from the lateral membrane of TJs. However, we observed no change in E-cadherin distribution. Analogous effects were seen with TcdA (data not shown). Redistribution of TJ proteins occurred in parallel with disorganization of F-actin and a fall in transepithelial resistance. Western blot analysis of whole-cell lysates from control and Tcd-incubated monolayers, however, did not show any difference in the total cellular concentrations of TJ proteins, suggesting that these proteins were not degraded (data not shown).

TcdB modulates the association of the TJ protein ZO-1 with the actin cytoskeleton. Since the actin cytoskeleton is central in regulation of TJ function and is itself regulated by Rho proteins, we determined the influence of TcdB on association of a TJ protein. ZO-1, with actin by coprecipitation experiments (17, 28, 29, 31). Actin immunoprecipiated from control (medium only) and TcdB-exposed monolayers was Western blotted with antibodies to the TJ cytoplasmic plaque protein ZO-1 and actin (Fig. 4). Only trace amounts of ZO-1 were detected in actin immunoprecipitates of toxin-treated cells. Actin was detectable in ZO-1 immunoprecipitates from toxin-treated cells, although at much reduced levels compared to those in untreated controls. Taken together, these results suggest that incubation of T84 monolayers with TcdB decreases the coprecipitation of ZO-1 with actin.

The association of TJ proteins with membrane rafts (DIGs) is modulated by TcdB. Biochemical properties of TJ-associated proteins such as occludin and ZO-1 include TX-100 insolubility, which has been attributed to either association of protein complexes with the cytoskeleton or protein oligomerization (54). Alternatively, TX-100 insolubility has been shown to be a property of proteins that partition to membrane microdomains also referred to as "rafts" or DIGs (2, 5, 18, 27). Utilizing differential detergent extraction and isopycnic sucrose density gradients, we recently documented a major pool of TJ proteins (HO and ZO-1) in raft-like membrane microdomains or DIGs (36). Since the Tcd toxins influenced paracellular permeability and TJ disassembly, we examined the effects of the above *C. difficile* toxins on association of TJ proteins with membrane rafts (Fig. 5 and 6). Control (medium only) and TcdB-exposed (80 $ng \cdot ml^{-1}$ for 2 h) epithelial monolayers were scraped into buffer containing 1% TX-100, and low-density TX-100 insoluble complexes physically akin to membrane rafts were isolated by floatation on linear 5 to 30% (wt/wt) sucrose density gradients. In agreement with other reports (5, 41), light density fractions containing TX-100-insoluble complexes (density of 1.08 g/cm^3) with light-scattering properties and enrichment in alkaline phosphatase activity were isolated (Fig. 5). Alkaline phosphatase has been used as a marker of plasma membranes and due, to its glycosylphosphatidylinositol linkage, resides in membrane microdomains with characteristics of membrane rafts or DIGs. As can be seen in Fig. 5, the light-scattering and alkaline phosphatase profiles were not significantly influenced by preexposure of epithelial cells to the TcdB toxin, suggesting that the toxin did not grossly alter the overall DIG characteristics. However, as shown in Fig. 6, disassembly of TJs induced by TcdB incubation markedly influenced the recovery of ZO-1 and HO (72 to 79 kDa) in the DIG fractions. In particular, HO was significantly reduced and ZO-1 was displaced from the low-density fractions to the bottom of the gradient (high-density fractions) (Fig. 6). Furthermore the above toxin-induced effects were TJ specific since TcdB treatment did not influence the partitioning of E-cadherin, a major component of the subjacent AJ. Analogous studies were performed to examine the influence of TcdA, and similar results were obtained (data not shown).

Effects of Tcd on the ultrastructure of TJs. Ultrastructural studies were undertaken to analyze influence of the *C. difficile* toxins on TJs. In agreement with our immunofluorescence results, treatment of T84 monolayers with TcdAB resulted in

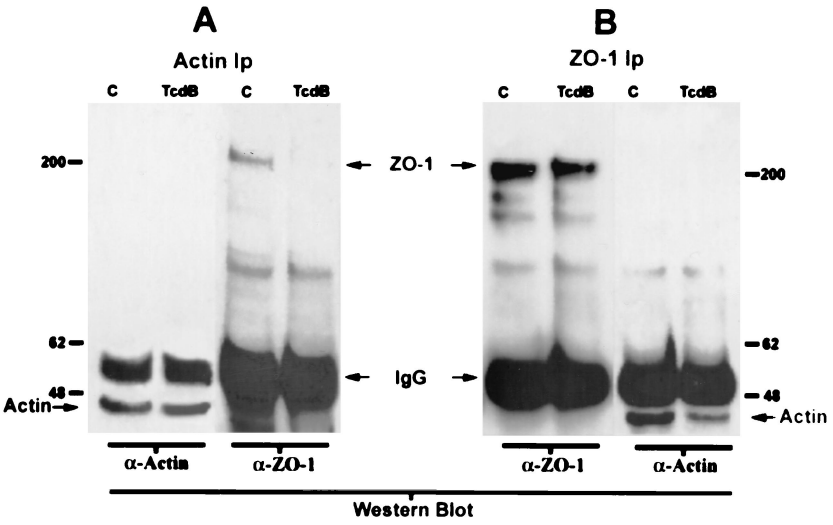

FIG. 4. Decreased coprecipitation of ZO-1 and actin following *C. difficile* toxin exposure. Actin (A) and ZO-1 (B) were immunoprecipitated (Ip) from control (lanes C) and TcdB (80 ng/ml for 2 h)-exposed (lanes TcdB) monolayers as detailed in Materials and Methods. Immunoprecipitated proteins were Western blotted with antibodies to ZO-1 or actin. Note the diminished ZO-1 level in actin immunoprecipitates following inactivation of Rho proteins with TcdB (arrow). Conversely, ZO-1 immunoprecipitates were probed with antibodies to ZO-1 and actin. Note the decreased intensity actin band in panel B (arrow). The band representing immunoglobulin G is marked as such (IgG). Representative data from three individual experiments are shown.

alteration of TJ ultrastructure (Fig. 7). Specifically, the peak Tcd-induced increase in paracellular permeability at a 2-h time point was accompanied by an initial loss of TJ membrane fusions ("kisses") and subsequently by complete loss of TJ architecture.

Since a subpopulation of DIGs contain a transmembrane scaffolding protein, caveolin (reviewed in reference 18 and by R. G. Parton and K. Simons, Comment, Science **269:** 1398–1399. 1995), that ocally colocalizes with occludin (36), we examined the influence of TcdB on the occludin-caveolin association in TJs by immunogold labeling and electron microscopy (Fig. 7, panels II). As can be seen, TcdB-induced TJ disassembly was associated with internalization of occludin (larger [15-nm] gold particles) from the lateral

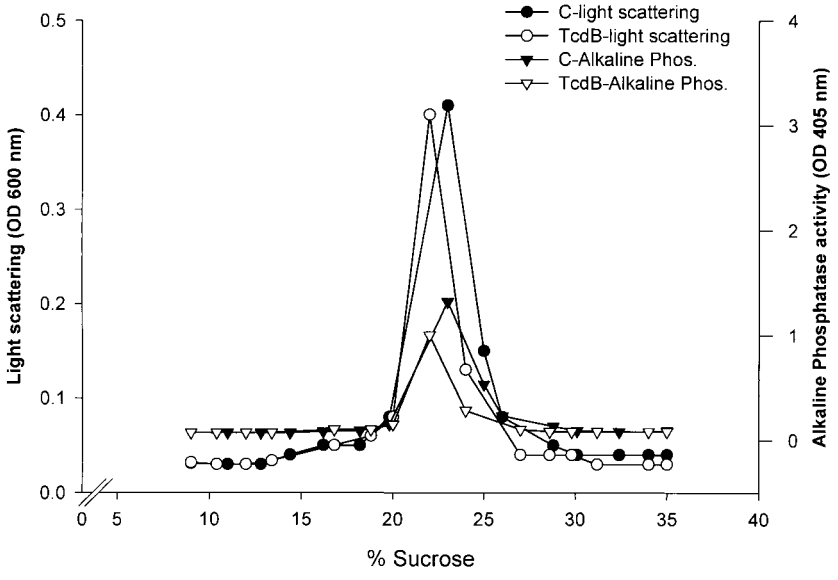

FIG. 5. Influence of TcdB on association of TJ proteins with "raft like" membrane microdomains: Control (medium only) (C) and TcdB-exposed epithelial monolayers (90 cm^2/condition) were isolated at 4°C in the presence of 1% TX-100 and separated in a linear 5 to 30% (weight/weight) sucrose gradient, and 0.5-ml fractions were analyzed. The profiles of light scattering at an optical density of 600 nm (OD 600 nm) and membrane alkaline phosphatase activity of the gradient fractions are shown. TX-100-insoluble complexes in 22% ± 2% sucrose (1.08 g/cm^3) from control monolayers of cells exhibit peak light scattering at 600 nm and have prominent alkaline phosphatase activity. Significant changes in these profiles were not observed following incubation with TcdB for 2 h. Representative data from three individual experiments are shown.

membrane, consistent with the immunofluorescence results. Interestingly, occludin is seen in association with membranous structures containing caveolin-1 (small [10-nm] gold particles). These membranous structures are reminiscent of caveolin-containing DIGs (45). Other areas were also identified where complete internalization of occludin was observed. Internalization of occludin from the lateral membrane in membranous structures in this manner could possibly implicate DIGs as a mechanism by which occludin could be recycled to the TJ membrane during the assembly of TJs.

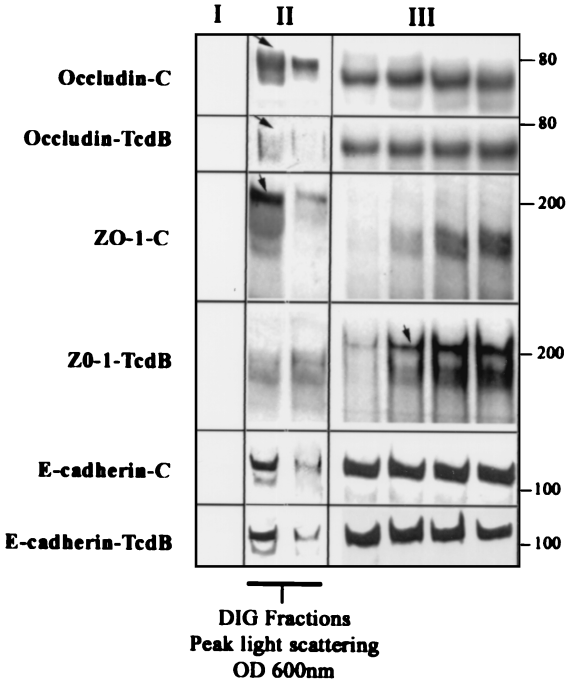

FIG. 6. *C. difficile* toxin B influences the distribution of TJ proteins occludin and ZO-1 in TX-100-insoluble raft-like membrane microdomains. Sucrose gradient fractions from epithelial monolayers described in the legend to Fig. 5 were analyzed by immunoblotting for the TJ proteins occludin and ZO-1. Lanes I, II, and III represent fractions taken from the top of the gradient (<20% sucrose, one lane shown), peak light-scattering fractions (~22% sucrose containing DIG fractions, two lanes shown), and representative fractions from the bottom of the gradients (>30% sucrose, four lanes shown), respectively. For occludin distribution; multiple bands ranging from 65 to 79 kDa were observed. While the low-molecular-mass species (~65 to 71 kDa) was distributed in both the low- and high-density sucrose fractions, the high-molecular-mass species (~72 to 79 kDa [arrow]) was observed in the low-density (~22 to 24%) TX-100-insoluble sucrose fractions. Preexposure of epithelial monolayers to TcdB and disassembly of TJs resulted in a decrease in high-molecular-mass occludin in the light-scattering fractions. For ZO-1 distribution, Western blots of gradient fractions from control epithelial monolayers revealed a major pool of recoverable ZO-1 in raft-containing low-density fractions (panel II, arrow) compared to the high-density fractions in the bottom of the gradient. Following exposure to TcdB (80 ng/ml for 2 h), ZO-1 redistributed predominantly to the high-density sucrose fractions (panel III, arrow). A broad nonspecific band at ~150 to 170 kDa that does not represent ZO-1 staining was observed with the Zymed polyclonal antibody raised to a ZO-1 fusion protein. E-cadherin was distributed in both the low-density (panel II) and high-density (panel III) fractions, a pattern that was not influenced by the Tcd toxin. The above results are representative results from four individual experiments. OD 600nm, optical density at 600 nm.

DISCUSSION

C. difficile TcdA and TcdB are UDP-glucosyltransferases that inactivate the Rho family of small GTPases by their ability to monoglucosylate these proteins. These toxins have a profound influence on the epithelial lining of the intestine and are associated with the common disorder pseudomembranous colitis. In this condition, colonic colonization by *C. difficile* results in profuse diarrhea that correlates with the presence of yellow plaques or pseudomembranes on the colonic mucosal surface. Histologically, there is severe acute inflammation with crypt destruction and abundant epithelial damage. The composition of pseudomembranes consists of polymorphonuclear leukocytes, fibrin, and cellular debris released from the affected mucosa. In this report, we document TcdAB-induced disruption of TJ structure and function that is likely to be an early event in epithelial damage induced by these toxins. In particular, we demonstrate that *C. difficile* toxin incubation results in decreased association of ZO-1 with the actin cytoskeleton and with TX-100-insoluble membrane microdomains. Such changes are accompanied by a diminished pool of high-molecular-weight occludin and internalization of occludin from the lateral TJ membrane.

The purified *C. difficile* toxins A and B used in our studies mediate global changes in F-actin architecture in both the apical and basal poles of T84 epithelial cells. The apical perijunction F-actin ring affiliates and regulates TJ function (29, 32). Thus, it is not surprising that disruption of this F-actin pool is associated with enhanced paracellular permeability. We have previously utilized C3 transferase from *Clostridium botulinum* to examine Rho protein function in intestinal epithelial cells. C3 transferase specifically ADP-ribosylates Rho, thereby influencing Rho effector coupling. Unlike the *C. difficile* toxins A and B, C3 does not modify other members of the Rho family, Rac and Cdc42. In our system, C3 transferase influences only the apical pool of F-actin in addition to inducing enhanced paracellular permeability and redistribution of ZO-1 (34). The results of our studies with the *C. difficile* and C3 toxins are in agreement with the results of studies of other cell types documenting a central role of Rho proteins in organizing polarized complexes of F-actin (22, 23). Taken together, these results support the concept that the Rho family of GTP binding proteins are central in determining the organization of F-actin and TJs in epithelial cells.

In addition to the prominent reorganization of F-actin, exposure of our epithelial monolayers to *C. difficile* toxins results in disruption of TJs and reduced association of ZO-1 with actin. The molecular mechanisms that underlie these prominent changes are not clear. Disorganization of apical F-actin and disruption of TJ function and structure occur in the same time frame. Such results provide additional support to the notion that the apical F-actin–TJ link is vital for regulation of paracellular permeability in epithelial cells.

Recent studies suggest organization of HO and ZO-1 in membrane raft-like structures, also referred to as DIGs, which are central to TJ function (36). Features of these microdomains include TX-100 insolubility, a buoyant density of ~1.08

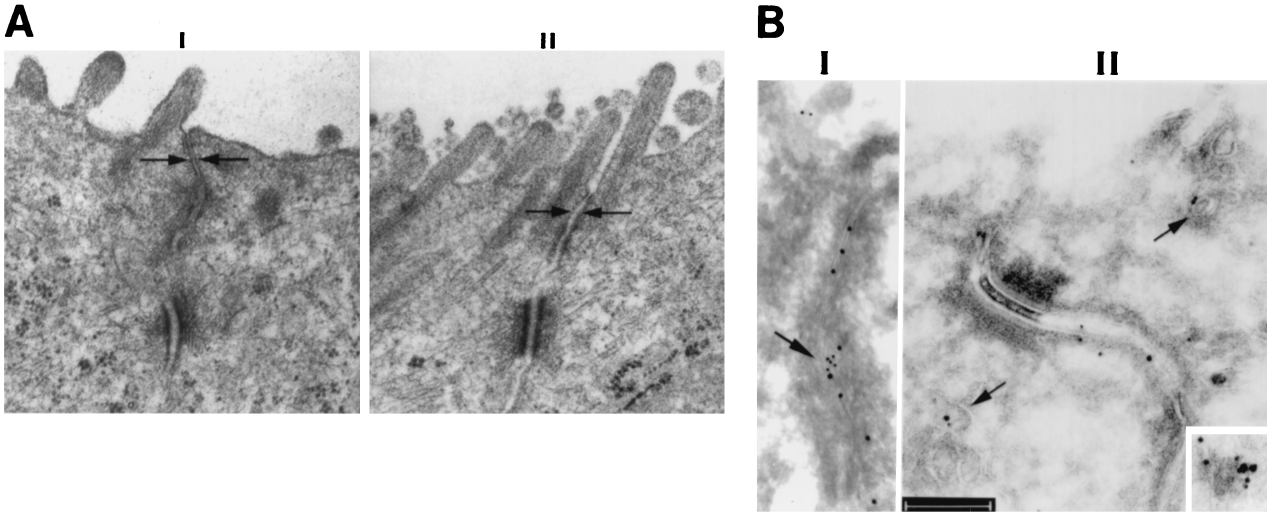

FIG. 7. Modulation of TJ structure by TcdB. Electron microscopic analysis of epithelial monolayers incubated in the presence and absence of TcdB is shown. (A) The representative micrographs illustrate an intact TJ in control cells (I) and a disrupted TJ with loss of membrane kisses following TcdB exposure (II). (B) Ultrastructural distribution of occludin and caveolin-1 following TcdB exposure. The ultrastructural distribution of occludin and caveolin 1 was determined by immunogold labeling and electron microscopy. The distribution of occludin and caveolin-1 is shown by the 15- and 10-nm gold particles, respectively. Panel I shows a normal distribution of occludin and caveolin-1 in the TJ lateral membrane (arrow). Following incubation with the TcdB toxin, these proteins are internalized from the lateral membrane of the TJ (panel II). Colocalization of these proteins inside the cells is observed along membranous structures (arrows). This is further highlighted in the inset (right lower corner). Bar, 200 nm.

g/cm^3, and enrichment in sphingolipids and cholesterol. Such DIG-like membrane microdomains appear to be central in many signaling pathways that originate from the cell surface (2, 27, 41). These compartments are enriched in a diverse array of signal transduction proteins. Thus, given the dynamic regulation of TJs, it is not surprising that its structural components are enriched in raft-like membrane microdomains. We had hypothesized that TJs contain numerous DIG-like membrane microdomains that constitute the sealing elements of TJs. Association of DIG proteins with the underlying actin cytoskeleton could act to organize TJ DIGs in beaded, linear assemblies, such as observed in freeze fracture electron microscopy (3, 16, 42, 46). The diminished association of occludin and ZO-1 with DIG-like membrane microdomains after exposure to TcdB supports a role of the Rho family of proteins in maintaining an affiliation of TJ proteins with such membrane microdomains.

In summary, from these data and those of others, it can be inferred that TcdA and TcdB mediate their effects on TJ structure and function via inactivation of Rho proteins. We demonstrate that exposure of epithelial monolayers to TcdA and TcdB results in disruption of both TJs and the actin cytoskeleton in parallel with a reduction in the association of ZO-1 with actin. It is clear that the apical aspect of the actin cytoskeleton is central in the regulation of TJ structure and function (28, 31, 33). Furthermore, the apical pool of F-actin is regulated by Rho proteins, as has been shown for Rho using C3 transferase (34). Since it is well established that TcdA and TcdB also specifically inactivate Rho protein family members by monoglucosylation (24, 25, 50), it is reasonable to assume that the effects of the toxin on apical actin structure and TJ morphology may result from Rho inactivation. However, since TcdAB also inactivate other Rho-related proteins, the contribution of these additional Rho family members to TJ structure and function is less clear. A better understanding of molecular mechanisms of TcdAB will provide insights into the role of small GTP binding proteins in barrier function and the pathophysiology of pseudomembranous colitis.

ACKNOWLEDGMENTS

We thank C. Foley for his expert technical assistance.

These studies were supported by National Institute of Health grants DK02130, DK53202, DK35932, DK55679, HL54229, and HL60540 and by Deutsche Forschungsgemeinschaft grants DFG Ei206/8-2 and g-2 to C.V.E.

REFERENCES

1. **Aktories, K.** 1997. Bacterial toxins that target Rho proteins. J. Clin. Investig. **99:**827–829.
2. **Anderson, R. G.** 1993. Caveolae: where incoming and outgoing messengers meet. Proc. Natl. Acad. Sci. USA. **90:**10909–10913.
3. **Balda, M. S., M. B. Fallon, C. M. Van Itallie, and J. M. Anderson.** 1992. Structure, regulation, and pathophysiology of tight junctions in the gastrointestinal tract. Yale J. Biol. Med. **65:**725–735, 737–740.
4. **Brown, D. A., and E. London.** 1997. Structure of detergent-resistant membrane domains: does phase separation occur in biological membranes? Biochem. Biophys. Res. Commun. **240:**1–7.
5. **Brown, D. A., and J. K. Rose.** 1992. Sorting of GPI-anchored proteins to glycolipid-enriched membrane subdomains during transport to the apical cell surface. Cell **68:**533–544.
6. **Chaves-Olarte, E., M. Weidmann, C. Eichel-Streiber, and M. Thelestam.** 1997. Toxins A and B from Clostridium difficile differ with respect to enzymatic potencies, cellular substrate specificities, and surface binding to cultured cells. J. Clin. Investig. **100:**1734–1741.
7. **Chun, M., U. K. Liyanage, M. P. Lisanti, and H. F. Lodish.** 1994. Signal transduction of a G protein-coupled receptor in caveolae: colocalization of endothelin and its receptor with caveolin. Proc. Natl. Acad. Sci. USA. **91:** 11728–11732.
8. **Ciesla, W. P., Jr., and D. A. Bobak.** 1998. Clostridium difficile toxins A and B are cation-dependent UDP-glucose hydrolases with differing catalytic activities. J. Biol. Chem. **273:**16021–16026.
9. **Denker, B. M., C. Saha, S. Khawaja, and S. K. Nigam.** 1996. Involvement of a heterotrimeric G protein alpha subunit in tight junction biogenesis. J. Biol. Chem. **271:**25750–25753.

10. **Dillon, S. T., E. J. Rubin, M. Yakubovich, C. Pothoulakis, J. T. LaMont, L. A. Feig, and R. J. Gilbert.** 1995. Involvement of Ras-related Rho proteins in the mechanisms of action of *Clostridium difficile* toxin A and toxin B. Infect. Immun. **63:**1421–1426.
11. **Fanning, A. S., B. J. Jameson, L. A. Jesaitis, and J. M. Anderson.** 1998. The tight junction protein ZO-1 establishes a link between the transmembrane protein occludin and the actin cytoskeleton. J. Biol. Chem. **273:**29745–29753.
12. **Friedrichson, T., and T. V. Kurzchalia.** 1998. Microdomains of GPI-anchored proteins in living cells revealed by crosslinking. Nature **394:**802–805.
13. **Furuse, M., T. Hirase, M. Itoh, A. Nagafuchi, S. Yonemura, S. Tsukita, and S. Tsukita.** 1993. Occludin: a novel integral membrane protein localizing at tight junctions. J. Cell Biol. **123:**1777–1788.
14. **Furuse, M., M. Itoh, T. Hirase, A. Nagafuchi, S. Yonemura, S. Tsukita, and S. Tsukita.** 1994. Direct association of occludin with ZO-1 and its possible involvement in the localization of occludin at tight junctions. J. Cell Biol. **127:**1617–1626.
15. **Furuse, M., H. Sasaki, K. Fujimoto, and S. Tsukita.** 1998. A single gene product, claudin-1 or -2, reconstitutes tight junction strands and recruits occludin in fibroblasts. J. Cell Biol. **143:**391–401.
16. **Gumbiner, B.** 1987. Structure, biochemistry, and assembly of epithelial tight junctions. Am. J. Physiol. **87:**C749–C758.
17. **Hall, A.** 1998. Rho GTPases and the actin cytoskeleton. Science **279:**509–514.
18. **Harder, T., and K. Simons.** 1997. Caveolae, DIGs, and the dynamics of sphingolipid-cholesterol microdomains. Curr. Opin. Cell Biol. **9:**534–542.
19. **Hecht, G., A. Koutsouris, C. Pothoulakis, J. T. LaMont, and J. L. Madara.** 1992. *Clostridium difficile* toxin B disrupts the barrier function of T84 monolayers. Gastroenterology **102:**416–423.
20. **Hecht, G., C. Pothoulakis, J. T. Lamont, and J. L. Madara.** 1988. *Clostridium difficile* toxin A perturbs cytoskeletal structure and tight junction permeability of cultured human intestinal epithelial monolayers. J. Clin. Investig. **56:**1053–1061.
21. **Jesaitis, L. A., and D. A. Goodenough.** 1994. Molecular characterization and tissue distribution of ZO-2, a tight junction protein homologous to ZO-1 and the *Drosophila* discs-large tumor suppressor protein. J. Cell Biol. **124:**949–961.
22. **Jou, T. S., and W. J. Nelson.** 1998. Effects of regulated expression of mutant RhoA and Racl small GTPases on the development of epithelial (MDCK) cell polarity. J. Cell Biol. **142:**85–100.
23. **Jou, T. S., E. E. Schneeberger, and W. J. Nelson.** 1998. Structural and functional regulation of tight junctions by RhoA and Racl small GTPases. J. Cell Biol. **142:**101–115.
24. **Just, I., G. Fritz, K. Aktories, M. Giry, M. R. Popoff, P. Boquet, S. Hegenbarth, and C. von Eichel-Streiber.** 1994. Clostridium difficile toxin B acts on the GTP-binding protein Rho. J. Biol. Chem. **269:**10706–10712.
25. **Just, I., M. Wilm, J. Selzer, G. Rex, C. von Eichel-Streiber, M. Mann, and K. Aktories.** 1995. The enterotoxin from *Clostridium difficile* (ToxA) monoglucosylates the Rho proteins. J. Biol. Chem. **270:**13932–13936.
26. **Kaoutzani, P., C. A. Parkos, C. Delp-Archer, and J. L. Madara.** 1993. Isolation of plasma membrane fractions from the intestinal epithelial model T84. Am. J. Physiol. **264:**C1327–C1335.
27. **Lisanti, M. P., P. E. Scherer, J. Vidugiriene, Z. Tang, A. Hermanowski-Vosatka, Y. H. Tu, R. F. Cook, and M. Sargiacomo.** 1994. Characterization of caveolin-rich membrane domains isolated from an endothelial-rich source: implications for human disease. J. Cell Biol. **126:**111–126.
28. **Madara, J. L.** 1987. Intestinal absorptive cell tight junctions are linked to cytoskeleton. Am. J. Physiol. **253:**C171–C175.
29. **Madara, J. L.** 1988. Tight junction dynamics: is paracellular transport regulated? Cell **53:**497–498.
30. **Madara, J. L., S. P. Colgan, A. Nusrat, C. Delp, and C. A. Parkos.** 1992. A simple approach to measurement of electrical parameters of cultured epithelial monolayers: use in assessing neutrophil epithelial interactions. J. Tissue Culture Methods **14:**209–216.
31. **Madara, J. L., R. Moore, and S. Carlson.** 1987. Alteration of intestinal tight junction structure and permeability by cytoskeletal contraction. Am. J. Physiol. **253:**C854–C861.
32. **Madara, J. L., J. Stafford, D. Barenberg, and S. Carlson.** 1988. Functional coupling of tight junctions and microfilaments in T84 monolayers. Am. J. Physiol. **254:**G416–G423.
33. **Madara, J. L., J. Stafford, K. Dharmsathaphorn, and S. Carlson.** 1987. Structural analysis of a human intestinal epithelial cell line. Gastroenterology **92:**1133–1145.
34. **Nusrat, A., M. Giry, J. R. Turner, S. P. Colgan, C. A. Parkos, D. Carnes, E. Lemichez, P. Boquet, and J. L. Madara.** 1995. Rho protein regulates tight junctions and perijunctional actin organization in polarized epithelia. Proc. Nat. Acad. Sci. USA. **92:**10629–10633.
35. **Nusrat, A., C. A. Parkos, A. E. Bacarra, P. J. Godowski, C. Delp-Archer, E. M. Rosen, and J. L. Madara.** 1994. Hepatocyte growth factor/scatter factor effects on epithelia. Regulation of intercellular junctions in transformed and nontransformed cell lines, basolateral polarization of c-met receptor in transformed and natural intestinal epithelia, and induction of rapid wound repair in a transformed model epithelium. J. Clin. Investig. **93:**2056–2065.
36. **Nusrat, A., C. A. Parkos, P. Verkade, C. S. Foley, T. W. Liang, W. Innis-Whitehouse, K. K. Eastburn, and J. L. Madara.** 2000. Tight junctions are membrane microdomains. J. Cell Sci. **113:**1771–1781.
37. **Parkos, C. A., S. P. Colgan, C. Delp, M. A. Arnaout, and J. L. Madara.** 1992. Neutrophil migration across a cultured epithelial monolayer elicits a biphasic resistance response representing sequential effects on transcellular and paracellular pathways. J. Cell Biol. **117:**757–764.
38. **Parkos, C. A., C. Delp, M. A. Arnaout, and J. L. Madara.** 1991. Neutrophil migration across a cultured intestinal epithelium: dependence on a CD11b/CD18-mediated event and enhanced efficiency in the physiologic direction. J. Clin. Investig. **88:**1605–1612.
39. **Riegler, M., R. Sedivy, C. Pothoulakis, G. Hamilton, J. Zacherl, G. Bischof, E. Cosentini, W. Feil, R. Schiessel, J. T. LaMont, et al.** 1995. *Clostridium difficile* toxin B is more potent than toxin A in damaging human colonic epithelium in vitro. J. Clin. Investig. **95:**2004–2011.
40. **Saitou, M., Y. Ando-Akatsuka, M. Itoh, M. Furuse, J. Inazawa, K. Fujimoto, and S. Tsukita.** 1997. Mammalian occludin in epithelial cells: its expression and subcellular distribution. Eur. J. Cell Biol. **73:**222–331.
41. **Sargiacomo, M., M. Sudol, Z. Tang, and M. P. Lisanti.** 1993. Signal transducing molecules and glycosyl-phosphatidylinositol-linked proteins form a caveolin-rich insoluble complex in MDCK cells. J. Cell Biol. **122:**789–807.
42. **Schneeberger, E. E., and R. D. Lynch.** 1992. Structure, function, and regulation of cellular tight junctions. Am. J. Physiol. **262:**L647–L661.
43. **Schnitzer, J. E., D. P. McIntosh, A. M. Dvorak, J. Liu, and P. Oh.** 1995. Separation of caveolae from associated microdomains of GPI-anchored proteins. Science **269:**1435–1439.
44. **Shapiro, M., J. Mattews, G. Hecht, C. Delp, and M. J. L.** 1991. Stabilization of F-actin prevents cyclic AMP-elicited C1 secretion in T84 cells. J. Clin. Investig. **87:**1903–1909.
45. **Simons, K., and E. Ikonen.** 1997. Functional rafts in cell membranes. Nature **387:**569–572.
46. **Stevenson, B. R., J. M. Anderson, and S. Bullivant.** 1988. The epithelial tight junction: structure, function and preliminary biochemical characterization. Mol. Cell. Biochem. **83:**129–145.
47. **Stevenson, B. R., and D. A. Goodenough.** 1984. Zonulae occludentes in junctional complex-enriched fractions from mouse liver: preliminary morphological and biochemical characterization. J. Cell Biol. **98:**1209–1221.
48. **Tsukita, S., and M. Furuse.** 1999. Occludin and claudins in tight-junction strands: leading or supporting players? Trends Cell Biol. **9:**268–273.
49. **Varma, R., and S. Mayor.** 1998. GPI-anchored proteins are organized in submicron domains at the cell surface. Nature **394:**798–801.
50. **von Eichel-Streiber, C., P. Boquet, M. Sauerborn, and M. Thelestam.** 1996. Large clostridial cytotoxins—a family of glycosyltransferases modifying small GTP-binding proteins. Trends Microbiol. **4:**375–382.
51. **von Eichel-Streiber, C., U. Harperath, D. Bosse, and U. Hadding.** 1987. Purification of two high molecular weight toxins of *Clostridium difficile* which are antigenically related. Microb. Pathog. **2:**307–318.
52. **Weber, E., G. Berta, A. Tousson, P. St John, M. W. Green, U. Gopalokrishnan, T. Jilling, E. J. Sorscher, T. S. Elton, D. R. Abrahamson, et al.** 1994. Expression and polarized targeting of a rab3 isoform in epithelial cells. J. Cell Biol. **125:**583–594.
53. **Wolf, A. A., M. G. Jobling, S. Wimer-Mackin, M. Ferguson-Maltzman, J. L. Madara, R. K. Holmes, and W. I. Lencer.** 1998. Ganglioside structure dictates signal transduction by cholera toxin and association with caveolae-like membrane domains in polarized epithelia. J. Cell Biol. **141:**917–927.
54. **Wong, V.** 1997. Phosphorylation of occludin correlates with occludin localization and function at the tight junction. Am. J. Physiol. **273:**C1859–C1867.

Editor: J. T. Barbieri